Supplemental Material

Supplemental Methods

Animal Models

The procedures followed were in accordance with approved guidelines set by the Animal Care Committee at the University of Missouri. Heterozygote control mice (m $Lepr^{db}$) (Background Strain: C57BLKS/J), and homozygote type 2 diabetic mice ($Lepr^{db}$) (Background Strain: C57BLKS/J) were purchased from Jackson Laboratory and maintained on a normal rodent chow diet. Male, 20-35g m $Lepr^{db}$, and 40-60 g $Lepr^{db}$ mice were used in this study. At the age of 12 to 16 weeks, m $Lepr^{db}$ mice were treated with murine recombinant IFNγ (R&D, 330 μg/kg/day, i.p. injection, 5 days).[1]

Improved Gastric Bypass Surgery

Improved gastric bypass surgery (IGBS) was performed using a modified surgical method that mimics the traditional Roux-en-Y gastric bypass surgery[2] (Supplemental Figure I). Food was restricted for 16 hours before surgery. The skin was prepared after anesthesia. Mice were anesthetized with sodium pentobarbital (50 mg/kg i.p. injection). The stomach and small intestine were exposed from the abdominal cavity, 15 cm away from Treitz ligament, and prepared for anastomosis. The small intestine and large curve of the stomach were anastomosed with 6-0 silk suture side to side. The pylorus was separated and the two parts of the pylorus were dissected and closed. The abdominal cavity was washed with warm 0.9% saline and the abdominal cavity was closed. Penicillin G (50,000 U/kg) was injected subcutaneously after surgery to prevent infection. The animals were fed a normal diet during recovery. In the sham surgery, the abdominal cavity was opened, but no further surgical procedures were performed. The cage was cleaned daily to reduce risk of infection and body

weight was measured every week until euthanasia. At age 12 weeks, m $Lepr^{db}$ and $Lepr^{db}$ mice were treated with either sham surgery or IGBS. $Lepr^{db}$ mice were assessed at 5, 10, 20, and 30 days post IGBS (P5, P10, P20, and P30), or 20 days after sham surgery. m $Lepr^{db}$ mice were assessed 20 days after either sham surgery or IGBS.

Body Weight, Abdominal Girth, Whole Body Fat Mass and Lean Mass Analysis

Body weight was determined using an electronic balance. Abdominal girth was measured with the use of a soft ruler. Whole body fat mass was determined using dual energy X-ray absorptiometry analysis (DEXA) methods. Briefly, a PIXImus small animal densitometer (GE Medical Systems; Waukesha, WI) was used to carry out DEXA. Mice were anesthetized with 2% isoflurane and subjected to 5 min DEXA scans at the beginning and end of the study. Analyses were carried out per manufacturer's instructions.[3]

Mesenteric Bed Weight and Adipocyte Size

The mesentery bed was rapidly separated from the intestine, and wet weight was determined. Freshly isolated mesenteric adipose tissue (MAT) was fixed in Z-fix, dehydrated and embedded in paraffin. The paraffin-embedded tissue was sectioned at 5 μm thickness, stained with hematoxylin and eosin, and then examined under a microscope (Olympus IX81, USA). The average size of adipocyte cells from each mouse was determined by analyzing 30-50 randomly-selected adipocytes from 2 sections using the Image J Software. [4]

Serum Concentration of Adiponectin

Serum adiponectin level was determined by a commercially available ELISA kit (Millipore). Values were expressed as micrograms per milliliter.

Western Blotting

10 mg of MAT, or 4-6 branches of small mesenteric arteries (SMA) were homogenized in lysis buffer (Cellytic™ MT Mammalian Tissue Lysis/Extraction Reagent, Sigma). Protein concentration was assessed using BCA™ Protein Assay Kit (Pierce), and equal amounts of protein were separated by SDS-PAGE and transferred to PVDF membranes (Biorad). Protein expression was detected using IFNγ primary antibody (Millipore), monocyte chemoattractant protein-1 primary antibody (MCP-1) (Abcam), or nitrotyrosine primary antibody (Abcam), Horseradish peroxidase-conjugated secondary antibodies were used. Signals were visualized by enhanced chemiluminescence (ECL, Santa Cruz), scanned densitometrically using Fuji LAS3000 and quantified with Multigauge software (Fujifilm). The relative amounts of protein expression were quantified to those of the corresponding m $Lepr^{db}$ control, which was set to a value of 1.0.[5]

Quantitative RT-PCR

Quantitative real-time PCR was done as previously reported with modification.[6] Briefly, total RNA was extracted from 10 mg of MAT using RNeasy Lipid Tissue Mini Kit (Qiagen), and 1.0 μg total RNA was processed directly to cDNA synthesis using the SuperScript™ III Reverse Transcriptase (Invitrogen). cDNA was amplified with the use of qRT-PCR Kit with SYBR® Green (Invitrogen). The primer sets for specific amplification of CD3, IFNγ, CD68, MCP-1, TNFα, MIP-1α and MIP-1β were designed by Primer3 software. Efficiency of the PCR reaction was determined using a dilution series of a standard MAT sample. The housekeeping gene β-actin was used for internal normalization. The mean threshold cycle (C_T) values for both the target (CD3, IFNγ, CD68 or MCP-1 etc.) and the internal control (β-actin) genes were determined. Data

were calculated by $2^{-\Delta\Delta CT}$ method ($\Delta\Delta CT=C_{T.\ target} - C_{T.\ \beta\text{-actin}}$).[7] Results was presented as fold change of transcripts for target normalized to internal control (β-actin), compared with m $Lepr^{db}$ (defined as 1.0 fold).

Immunohistochemistry

Analysis of inflammatory cells in MAT by Immunohistochemistry was done as previously reported.[8] Briefly, freshly isolated MAT was fixed in Z-fix, and embedded in paraffin. 5 μm sections were stained for rabbit anti-mouse CD3 (Abcam), rat anti-mouse Mac-3 (BD Biosciences), and rat anti-mouse F4/80 (Abcam), then incubated with appropriate biotinylated secondary antibodies followed by incubation with avidin-biotin complex (Vector). The reaction was visualized with 3-amino-9ethyl carbazole (DAKO). Sections were counterstained with Gill's hematoxylin solution (Sigma). [8]

Functional Assessment of Small Mesenteric Arteries

Isolated small mesenteric artery responses were studied using wire myograph as previously reported.[9] Briefly, first order of main branch of mesenteric arteries with internal diameter of 200 μm to 250 μm were cut into 2 mm long rings and mounted on Myograph 610M (A&D Instrument). The passive tension-internal circumference was determined by stretching to achieve an internal circumference equivalent to 60 % to 70 % of that of the blood vessel under a transmural pressure of 100 mmHg. Vessels were maintained in Physiological Saline Solution (PSS) bubbled with 95% O_2-5% CO_2 at 37 ºC for the remainder of the experiment. PSS contained 118.99 mM NaCl, 4.69 mM KCl, 1.18 mM KH_2PO4, 1.17 mM $MgSO_4 \bullet 7H_2O$, 2.50 mM $CaCl_2 \bullet 2H_2O$, 14.9 mM $NaHCO_3$, 5.5 mM D-Glucose, and 0.03 mM EDTA. After an equilibration period of 45 min, vessels were precontracted with 1 μmol/L phenylephrine (PE). A cumulative dose-

response curve was obtained by adding acetylcholine (ACh, 1 nmol/L to 10 μmol/L) and sodium nitroprusside (SNP, 1 nmol/L to 10 μmol/L). Relaxation at each concentration was measured and expressed as the percentage of force generated in response to PE.[9-10] NO availability was evaluated by ACh concentration-response curve repeated after incubation with the NO synthase inhibitor N-Nitro-L-arginine methyl ester (L-NAME, 100 μM, 20 min). PE-induced vasoconstriction was evaluated by cumulative addition of PE (1 nmol/L to 10 μmol/L). The contraction induced by PE was normalized to the maximal force of contraction induced by 120 mM of KCl.[10]

Measurement of Superoxide Using Electron Paramagnetic Resonance Spectroscopy

Measurement of superoxide using Electron Paramagnetic Resonance Spectroscopy (EPR) was performed as previously described from our laboratory.[5, 11] EPR spectra was determined from the MAT and SMA homogenates. In brief, a 10% tissue homogenate was prepared in a 50 mmol/L phosphate buffer containing 0.01 mmol/L EDTA. The homogenate was then subjected to low-speed centrifugation (1,000 g) for 10 min to remove unbroken cells and debris. The supernatants containing 2 mmol/L CPH (1-hydrox-3-carboxypyrrolidine) were incubated for 30 min at 37°C and frozen quickly in liquid nitrogen. Superoxide quantification from the EPR spectra was determined by double integration of the peaks, with reference to a standard curve generated from horse radish peroxidase generation of the anion from standard solutions of hydrogen peroxide using p-acetamidophenol as the co-substrate normalized by protein concentration.

Data Analysis

All data were presented as mean±SEM except as specifically stated. Statistical comparisons were performed with 2-way ANOVA for vasomotor responses under various treatments, and with one-way ANOVA for other data. Intergroup differences were tested with LSD inequality. Significance was accepted at $P < 0.05$.

Supplemental Results

Table I. Basic Parameters

	m Lepr^{db} Sham	m Lerp^{db} IGBS P20	Lepr^{db} Sham	Lepr^{db} IGBS P5	Lepr^{db} IGBS P10	Lepr^{db} IGBS P20	Lepr^{db} IGBS P30
Body Weight, Before, g	25.4±0.7	25.9±0.6	48.3±2.4*	50.0±2.5*	51.5±2.3*	49.3±2.5*	51.5±2.5*
Body Weight, After, g	26.7±1.5	22.9±2.2*	49.2±3.2*	43.4±3.2*$^{\#\&}$	42.1±1.7*$^{\#\&}$	41.2±1.8*$^{\#\&}$	40.5±2.1*$^{\#\&}$
Abdominal Girth, Before, cm	5.9±0.7	6.1±0.2	10.6±0.4*	10.8±0.4*	10.3±0.8*	10.4±0.8*	10.2±0.6*
Abdominal Girth, After, cm	6.3±0.5	6.0±0.2	11.0±0.6*	10.2±0.3*$^{\#\&}$	9.3±0.3*$^{\#\&}$	9.0±0.2*$^{\#\&}$	8.7±0.4*$^{\#\&}$
Lean Mass, Before, g	19.1±1.1	20.8±1.2	16.4±0.9*	16.0±1.7*	17.3±1.9*	15.7±1.3*	17.0±1.9*
Lean Mass, After, g	22.5±1.0$^{\&}$	20.2±2.3	16.1±1.4*	15.4±1.7*	15.3±1.4*	16.5±1.0*	17.0±1.3*
Fat Mass, Before, g	6.2±1.2	5.1±1.3	31.9±2.0*	34.1±1.9*$^{\#}$	34.2±0.9*$^{\#}$	33.6±2.3*$^{\#}$	34.6±1.2*$^{\#}$
Fat Mass, After, g	4.3±0.9	2.7±0.6$^{\&}$	33.1±3.0*	28.0±3.5*$^{\#\&}$	26.8±2.0*$^{\#\&}$	24.7±2.0*$^{\#\&}$	23.5±1.1*$^{\#\&}$
Blood Glucose, Before, mg/dl	109±12	117±15	450±35*	462±100*	517±49*	504±46*	465±50*
Blood Glucose, After, mg/dl	106±11	78±13	405±57*	215±78*$^{\#\&}$	162±55$^{\#\&}$	133±45$^{\#\&}$	189±71*$^{\#\&}$
Food Intake, Before, g	3.9±0.4	4.2±0.3	6.4±0.4*	6.4±0.4*	6.1±0.3*	6.3±0.5*	6.4±0.5*
Food Intake, After, g	4.2±0.3	4.0±0.2$^{\&}$	6.7±0.3*	4.8±0.8$^{\#\&}$	5.1±0.2*$^{\#\&}$	5.4±0.4*$^{\#\&}$	5.2±0.6*$^{\#\&}$

Table II. Mesenteric Bed Weight and Adipocyte Size

	Mesenteric Bed Weight, g	Adipocyte Size, μm^2
m Lepr^{db} Sham	0.161±0.009	943.432±69.026
m Lepr^{db} IGBS P20	0.134±0.016	952.223±26.997
Lepr^{db} Sham	1.493±0.061 *	5189.787±344.191 *
Lepr^{db} IGBS P5	1.269±0.068 *$^{\#}$	4885.988±301.041 *
Lepr^{db} IGBS P10	1.230±0.038 *$^{\#}$	4266.563±161.064 *$^{\#}$
Lepr^{db} IGBS P20	1.252±0.044 *$^{\#}$	4192.925±244.800 *$^{\#}$
Lepr^{db} IGBS P30	1.267±0.061 *$^{\#}$	4168.630±212.424 *$^{\#}$

Table III. Primer Sequences Used for Real-Time RT-PCR

Name	Accession #	Sequence	Target Length
IFNγ s	NM_008337	ACTGGCAAAAGGATGGTGAC	212
IFNγ as	NM_008337	GACCTGTGGGTTGTTGACCT	212
MCP-1 s	NM_011333	AGCACCAGCCAACTCTCACT	184
MCP-1 as	NM_011333	TCATTGGGATCATCTTGCTG	184
CD3 s	NM_007648	TCCCAACCCAGACTATGAGC	95
CD3 as	NM_007648	GCGATGTCTCTCCTATCTGTCA	95
CD68 s	NM_009853	TACCCAATTCAGGGTGGAAG	191
CD68 as	NM_009853	CTCGGGCTCTGATGTAGGTC	191
TNFα s	NM_013693	GTCCCCAAAGGGATGAGAAG	134
TNFα as	NM_013693	CACTTGGTGGTTTGCTACGA	134
MIP-1α s	NM_011337	GTGTAGAGCAGGGGCTTGAG	99
MIP-1α as	NM_011337	AGAGTCCCTCGATGTGGCTA	99
MIP-1β s	NM_013652	CCTGACCAAAAGAGGCAGAC	134
MIP-1β as	NM_013652	GAGGAGGCCTCTCCTGAAGT	134
β-actin s	NM_007393	GCTCTTTTCCAGCCTTCCTT	168
β-actin as	NM_007393	CTTCTGCATCCTGTCAGCAA	168

Figure I.

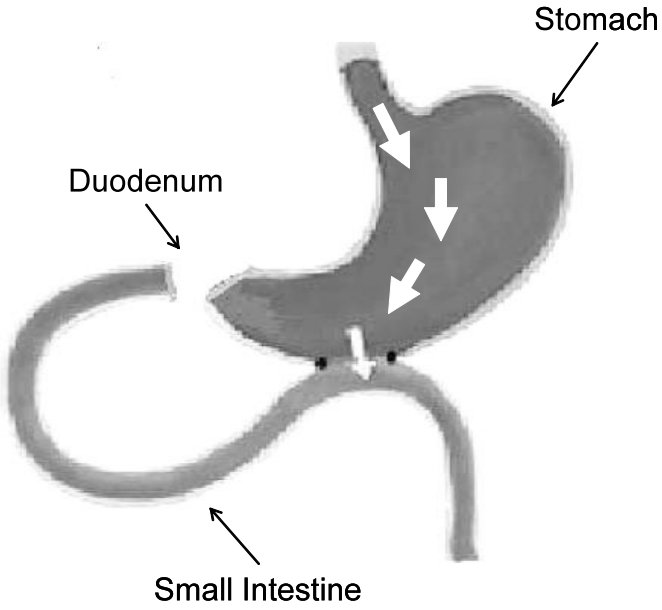

Figure II.

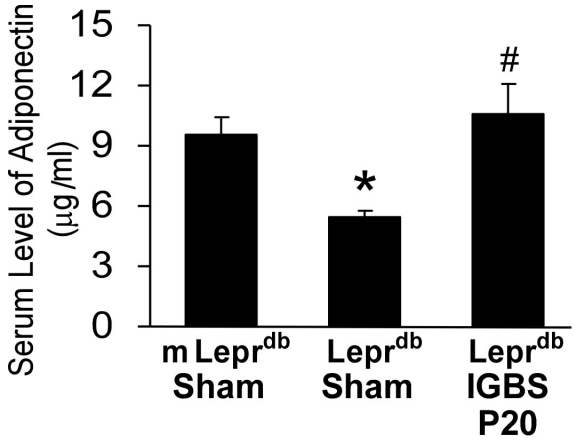

Figure III.

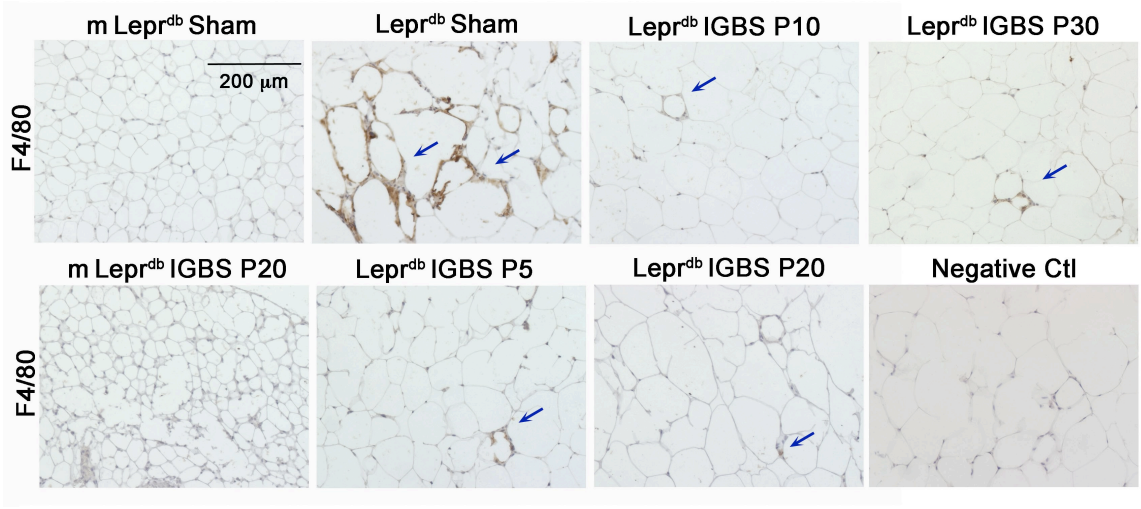

Figure IV.

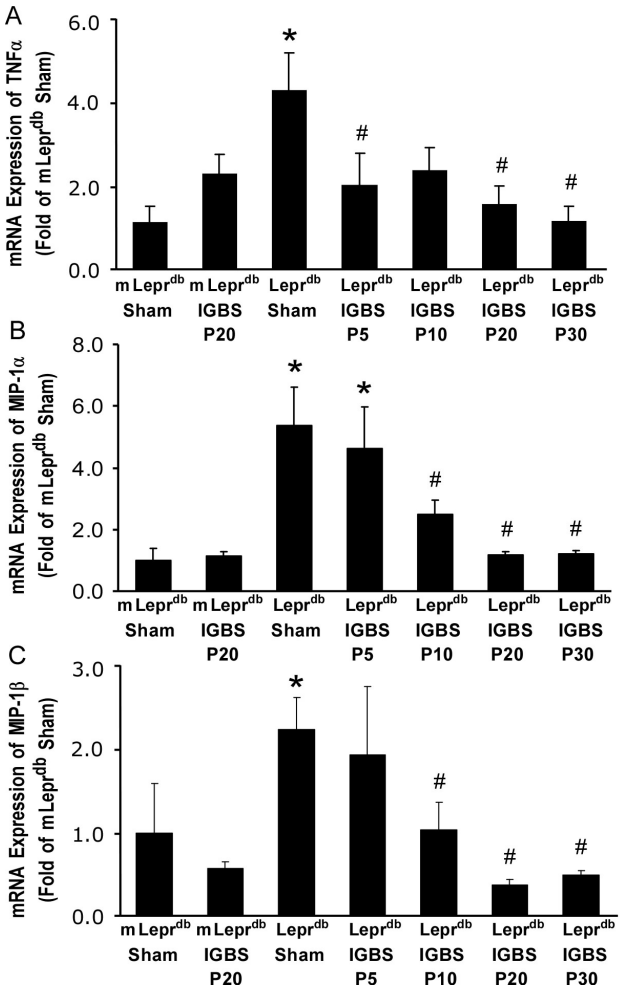

Figure V.

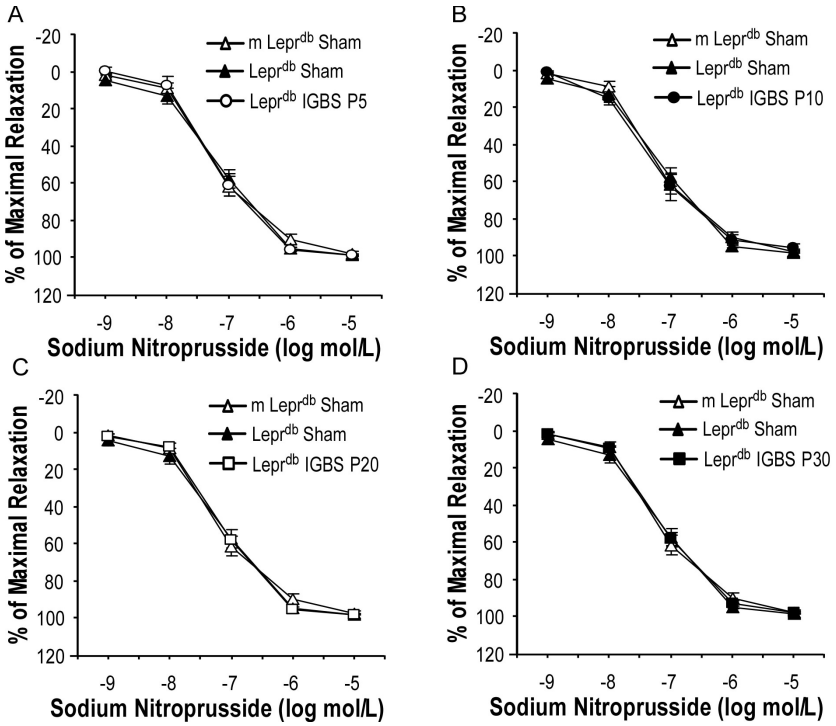

Figure VI.

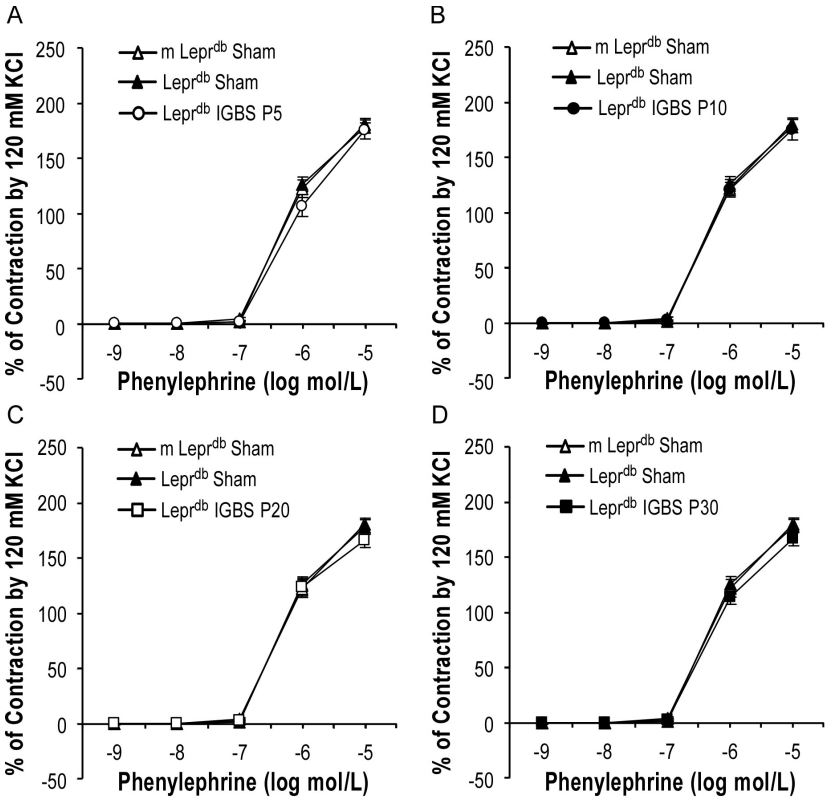

Figure VII.

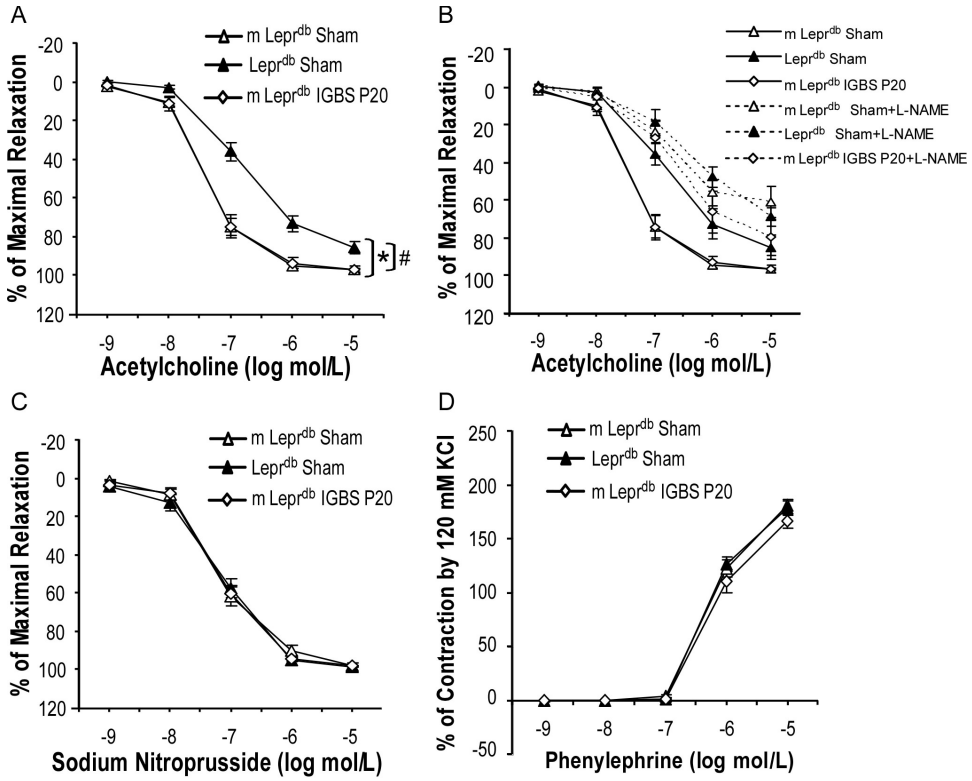
A
m Lepr^db Sham
Lepr^db Sham
m Lepr^db IGBS P20
% of Maximal Relaxation
-20
0
20
40
60
80
100
120
-9
-8
-7
-6
-5
Acetylcholine (log mol/L)
*
#
B
m Lepr^db Sham
Lepr^db Sham
m Lepr^db IGBS P20
m Lepr^db Sham+L-NAME
Lepr^db Sham+L-NAME
m Lepr^db IGBS P20+L-NAME
% of Maximal Relaxation
Acetylcholine (log mol/L)
C
m Lepr^db Sham
Lepr^db Sham
m Lepr^db IGBS P20
% of Maximal Relaxation
Sodium Nitroprusside (log mol/L)
D
m Lepr^db Sham
Lepr^db Sham
m Lepr^db IGBS P20
% of Contraction by 120 mM KCl
250
200
150
100
50
0
-50
Phenylephrine (log mol/L)

Table I. Basic Parameters

The body weight, abdominal girth, whole body fat mass and lean mass, blood glucose level, and food intake were examined before and after Improved Gastric Bypass Surgery (IGBS). IGBS decreased body weight, abdominal girth, whole body fat mass, blood glucose level and food intake in diabetic mice ($Lepr^{db}$) without remarkably affecting the lean mass. IGBS slightly reduced the body weight, fat mass and food intake in non-diabetic control mice (m $Lepr^{db}$), but did not significantly affect other parameters including abdominal girth, lean mass, and blood glucose level. Data represent mean±SEM. n=6 mice per group. * $P<0.05$ compared with m $Lepr^{db}$+Sham surgery; # $P<0.05$ compared with $Lepr^{db}$+Sham surgery; & $P<0.05$ compared with animals prior to IGBS.

Table II. Mesenteric Bed Weight and Adipocyte Size

IGBS decreased mesenteric bed weight and adipocyte size of MAT in $Lepr^{db}$ mice, but not in m $Lepr^{db}$ mice. Data represent mean±SEM. n=6-12 mice. *$P<0.05$ compared with m $Lepr^{db}$+Sham surgery; # $P<0.05$ compared with $Lepr^{db}$+Sham surgery.

Table III. Primer Sequences Used for Real-Time RT-PCR

Figure Legends

Figure I. Schematic figure showing the surgery procedure of improved gastric bypass surgery (IGBS). IGBS is a modified method from the traditional Roux-en-Y gastric bypass surgery. The small intestine and large curve of the stomach was anastomosed. The pylorus was separated and the two parts of the pylorus were dissected and closed. After IGBS, food

bypassed the pylorus and part of the small intestine and entered the distal part of the small intestine.

Figure II. IGBS increased the serum level of adiponectin in diabetic mice. Serum level of adiponectin was reduced in $Lepr^{db}$ vs. m $Lepr^{db}$ control. IGBS significantly increased the level of serum adiponectin at 20 days post surgery (IGBS P20). Data represent mean±SEM. n=4-6 mice. *P<0.05 compared with m $Lepr^{db}$+Sham surgery; # P<0.05 compared with $Lepr^{db}$+Sham surgery.

Figure III. Immunohistochemical staining of F4/80 positive macrophage. F4/80 positive macrophage infiltration in MAT was higher in $Lepr^{db}$+Sham surgery. IGBS reduced MAT macrophage infiltration. Data shown were representative of 4 separate experiments.

Figure IV. mRNA expression of TNFα, MIP-1α, and MIP-1β by quantitative RT-PCR. IGBS decreased mRNA expression of TNFα (A), MIP-1α (B), and MIP-1β (C) in MAT of $Lepr^{db}$ mice. Data represent mean±SEM, n=6-8 mice. *P<0.05 compared with m $Lepr^{db}$+Sham surgery; # P<0.05 compared with $Lepr^{db}$+Sham surgery. MIP, macrophage inflammatory protein.

Figure V. IGBS did not affect endothelium-independent vasorelaxation. Sodium nitroprusside (SNP)-induced endothelium-independent vasorelaxation of SMA was not statistically different among all groups. Data represent mean±SEM. n=4-18 mice.

Figure VI. IGBS did not affect vasoconstriction to phenylephrine. Phenylephrine (PE)-induced vasoconstriction of SMA was similar among all groups. Data represent mean±SEM. n=4-18 mice.

Figure VII. The effects of IGBS on m $Lepr^{db}$ control mice. IGBS did not affect ACh (A) and SNP (C)-induced vasorelaxation, or PE-induced vasoconstriction (D) of SMA in m

Lepr^{db} control mice. Data represent mean±SEM. n=4-18 mice. *P<0.05 compared with m Lepr^{db}+Sham surgery; # P<0.05 compared with Lepr^{db}+Sham surgery.

Reference

1. Jackson SH, Miller GF, Segal BH, Mardiney M, 3rd, Domachowske JB, Gallin JI, Holland SM. Ifn-gamma is effective in reducing infections in the mouse model of chronic granulomatous disease (cgd). *J Interferon Cytokine Res*. 2001;21:567-573
2. Troy S, Soty M, Ribeiro L, Laval L, Migrenne S, Fioramonti X, Pillot B, Fauveau V, Aubert R, Viollet B, Foretz M, Leclerc J, Duchampt A, Zitoun C, Thorens B, Magnan C, Mithieux G, Andreelli F. Intestinal gluconeogenesis is a key factor for early metabolic changes after gastric bypass but not after gastric lap-band in mice. *Cell Metab*. 2008;8:201-211
3. Johnston SL, Peacock WL, Bell LM, Lonchampt M, Speakman JR. Piximus dxa with different software needs individual calibration to accurately predict fat mass. *Obes Res*. 2005;13:1558-1565
4. Li Z, Zhang H, Denhard LA, Liu LH, Zhou H, Lan ZJ. Reduced white fat mass in adult mice bearing a truncated patched 1. *Int J Biol Sci*. 2008;4:29-36
5. Gao X, Belmadani S, Picchi A, Xu X, Potter BJ, Tewari-Singh N, Capobianco S, Chilian WM, Zhang C. Tumor necrosis factor-alpha induces endothelial dysfunction in lepr(db) mice. *Circulation*. 2007;115:245-254
6. Zhang H, Zhang J, Ungvari Z, Zhang C. Resveratrol improves endothelial function: Role of tnf{alpha} and vascular oxidative stress. *Arterioscler Thromb Vasc Biol*. 2009;29:1164-1171
7. Pfaffl MW. A new mathematical model for relative quantification in real-time rt-pcr. *Nucleic Acids Res*. 2001;29:e45

8. Whiteland JL, Nicholls SM, Shimeld C, Easty DL, Williams NA, Hill TJ. Immunohistochemical detection of t-cell subsets and other leukocytes in paraffin-embedded rat and mouse tissues with monoclonal antibodies. *J Histochem Cytochem*. 1995;43:313-320

9. Su J, Lucchesi PA, Gonzalez-Villalobos RA, Palen DI, Rezk BM, Suzuki Y, Boulares HA, Matrougui K. Role of advanced glycation end products with oxidative stress in resistance artery dysfunction in type 2 diabetic mice. *Arterioscler Thromb Vasc Biol*. 2008;28:1432-1438

10. Pannirselvam M, Wiehler WB, Anderson T, Triggle CR. Enhanced vascular reactivity of small mesenteric arteries from diabetic mice is associated with enhanced oxidative stress and cyclooxygenase products. *Br J Pharmacol*. 2005;144:953-960

11. Zhang C, Xu X, Potter BJ, Wang W, Kuo L, Michael L, Bagby GJ, Chilian WM. Tnf-alpha contributes to endothelial dysfunction in ischemia/reperfusion injury. *Arterioscler Thromb Vasc Biol*. 2006;26:475-480